ARTICLE

Protonation Effect on One- and Two-photon Absorption Property of a Newly Synthesized Octupolar Chromophore

Hong-juan Ding, Jie Sun, Chuan-kui Wang*

College of Physics and Electronics, Shandong Normal University, Ji'nan 250014, China

(Dated: Received on September 5, 2012; Accepted on September 27, 2012)

The protonation effects on one- and two-photon absorption properties of an octupolar molecule TA with 1,3,5-triazine core and pyrrole electron-donating end-groups have been studied at hybrid density functional theory level. A computational scheme is developed to simulate a proton attached to an atom. The numerical results show that large changes in both one- and two-photon absorption properties are observed when the compound is transformed from neutral to threefold protonated states. When the compound is protonated, more charge transfer states appear and the absorption band has a red-shift. Furthermore, the two-photon absorption cross-section is largely enhanced. The theoretical calculations demonstrate the protonation effect on promoting the intramolecular charge transfer strength. The results present qualitative agreement with the experimental observations. A two-photon absorption switch with the compound TA based on the protonation effect is proposed.

Key words: Protonation, Two-photon absorption, Response theory, Octupolar chromophore

I. INTRODUCTION

In recent years, organic materials with large two-photon absorption (TPA) cross-sections have been extensively investigated in both experimental and theoretical ways due to their potential applications in optical limiting [1−5], photodynamic therapy [6−10], up-converted lasing [11, 12], three-dimensional (3D) optical data storage [8, 13], and microfabrication [14−16]. These applications are possible just for specifically designed organic molecules with a large TPA cross-section. Thus, improving the TPA cross-section values of compounds is a fundamental issue in this field. Up to now, one has found that factors such as the conjugation length, the π center properties, the symmetrical or asymmetrical arrangement of electron-donor (D) and electron-acceptor (A) attached to the π center and their strength to push and pull electrons, coplanarity and the molecular dimensionality have a significant impact on TPA cross-sections [17]. However, the comprehensive understanding of TPA structure-property relationships is still limited.

The influence of the solvent on electronic and geometrical structures of compounds is an important aspect in the modeling of their optical properties since almost all experimental measurements for organic molecules have been carried out in the liquid phase or in solutions [18−24]. As one kind of solvent effect, protonation effect is a special one and has been extensively investigated in experiments [20, 21]. Moreover, this effect was used to design functional optical devices [22−24]. Asselberghs *et al.* have reported that reversible switching of the molecular second-order nonlinear optical (NLO) polarizability is achieved by means of proton-transfer [23]. Werts *et al.* have displayed large changes in both one-photon absorption (OPA) and TPA as well as fluorescence emission characteristics caused by the modulation upon protonation at the terminal phenolic hydroxyl and amino groups in quadripolar push-pull-push chromophores [21]. Recently, Liu *et al.* have successfully synthesized octupolar chromophore TA with a 1,3,5-triazine core and pyrrole electron-donating end-groups [24]. The experimental measurement revealed that its TPA cross-section is enhanced a lot upon threefold protonation.

However, only rare theoretical simulations have been focused on the effect of protonation because the treatment of protons in chromophores at first-principles level is a complicated issue. Up to now, the available theoretical works have used a crude model for dealing with protons, namely, a few positive charges are added in the whole molecule during the numerical simulation [24−26]. In order to descript the protonation effect precisely, we apply a computational scheme for dealing with protons. The protonation effects on OPA and TPA properties of the chromophores are thus analyzed at hybrid density functional theory (DFT) level.

*Author to whom correspondence should be addressed. E-mail: ckwang@sdnu.edu.cn, FAX: +86-531-86182521

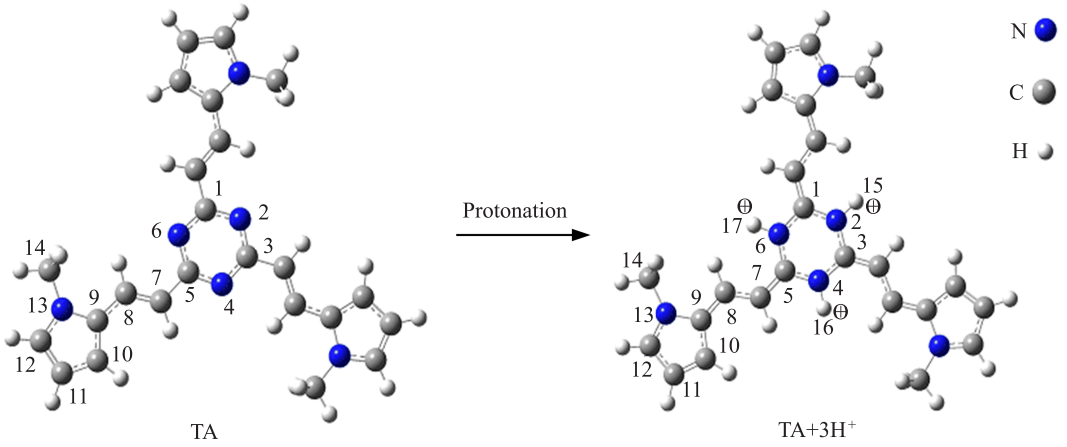

FIG. 1 Optimized geometries of the neutral TA and its threefold protonated state TA+3H$^+$.

II. COMPUTATIONAL DETAILS

The OPA probability and the TPA cross-section that can be directly compared with the experimental results are described in Ref.[27]. The geometrical structures are fully optimized using the Gaussion 03 package [28] at hybrid DFT level. The calculation of OPA is carried out by use of time-dependent density functional theory (TD-DFT) theory. The quadratic response theory implemented in the Dalton package [29] is used to calculate TPA cross-section of molecules, providing an analytical solution for the TPA cross-section.

Considering the protonation effect, we use a scheme to simulate a proton attached to an atom. In detail, in order to describe the protonation of a nitrogen atom, a hydrogen atom with a basis restricted to only the s orbital is used, and the exponent of the basis function is enlarged until there is hardly electronic in s orbital [30]. This treatment leaves the hydrogen atom almost charged with +|e|.

TABLE I Selective bond lengths of the optimized geometries for compounds TA and TA+3H$^+$.

	Selective bond length/pm	
	TA	TA+3H$^+$
C1−N2	134.8	136.6
N2−C3	133.9	137.5
C3−N4	134.8	136.6
N4−C5	133.9	137.5
C5−N6	134.8	136.6
N6−C1	133.9	137.5
C5−C7	145.8	138.2
C7−C8	135.0	140.5
C8−C9	143.6	138.0
C9−C10	139.5	143.5
C10−C11	140.7	137.0
C11−C12	138.4	141.8
C12−N13	136.6	133.3
N13−C9	139.1	141.5
N13−C14	145.5	146.6

III. RESULTS AND DISCUSSION

A. Molecular structures

We optimize the molecular geometries at the B3LYP/6-311+G(d,p) level. The geometries are shown in Fig.1. We can observe that the geometries of the neutral transient absorption (TA) and the protonated TA+3H$^+$ have C_3 symmetry. Some bond lengths of the optimized geometries for the neutral compound TA and protonated compound TA+3H$^+$ are listed in Table I. From Table I, one can find that the bond lengths in the 1,3,5-triazine core are extended by the protons. Moreover, the C−C bond lengths in the groups bridging the 1,3,5-triazine core and pyrrole end-group are changed a lot. For example, when the compound is changed from the neutral to protonated states, the bond length of C5−C7 is shortened from 145.8 pm to 138.2 pm, while the bond length of C7−C8 is lengthened from 135.0 pm to 140.5 pm.

In addition, net charge distributions for selective atoms of the TA and TA+3H$^+$ are listed in Table II. The protonation changes the net charge distributions obviously. When the compound is protonated, the C atoms in the triazine core own positive charge as much as +e, and the N atoms have net charge larger than −e. These amounts are quite larger than those for the case without protonation. However, the net charge of the whole triazine group has a little change from −0.04 e to 0.08 e after the protonation, although the sign is varied. Moreover, the net charges of C7 and pyrrole end-group are increased to −1.02 and 1.17 e respectively after the protonation, demonstrating an enhanced push-pull charge ability. As a result, the optical properties

DOI:10.1088/1674-0068/25/06/666-670

TABLE II The net charge distribution for selective atoms in compounds TA and TA+3H$^+$.

	Net charge distribution/e	
	TA	TA+3H$^+$
C1	0.018	1.173
N2	−0.038	−1.143
C3	0.023	1.168
N4	−0.037	−1.142
C5	0.027	1.171
N6	−0.037	−1.144
C7	−0.442	−1.018
C8	−0.161	−0.152
H15		0.998
H16		0.998
H17		0.998
Triazine core	−0.044	0.083
Pyrrole groups	0.616	1.167

are expected to have an obvious variation with the protonation. It is noted that the net charge of H15, (H16 or H17) is 0.998 e, demonstrating a reasonable and precise treatment on protons in our computational scheme.

B. One-photon absorption

The excitation energies and the oscillator strengths of the single-point excited states are calculated by the TD-DFT at the B3LYP/6-311+G(d,p) level with fully optimized geometries. The excitation energy, the corresponding wavelength and the oscillator strength (larger than 0.1) of the excited states are listed in Table III. The numerical results show that there are four charge-transfer (CT) states for neutral compound TA, namely, the forth, fifth, eleventh, and twelfth excited states. In addition, it is noted that the excitation energies and the oscillator strengths of the forth and the fifth (the eleventh and the twelfth) excited states are nearly the same, which are regarded as near-degenerate states. In comparison with the neutral TA, TA+3H$^+$ has two more CT states in the interested energy region, showing more CT channels caused by the protonation effect.

In order to clearly observe the OPA property in the lower energy region, we have carried out a Lorenz expansion of the oscillator strength at each excited state, and the so-called OPA spectra are shown in Fig.2. From Fig.2, one can see that there exists one more OPA peak located on a wavelength of 518 nm for the compound TA+3H$^+$ compared to the compound TA, which provides a new intramolecular charge transfer channel. Furthermore, the other two OPA peaks located on 418 and 318 nm for the TA+3H$^+$ have an obvious red-shift. The theoretical results show the main features of the OPA properties of the protonated compound found in experiments. The more CT states and the red-shift of

TABLE III The oscillator strength $\delta_{\rm op}$, the excitation energies E, and the corresponding wavelength $\lambda_{\rm op}$ of the excited states with $\delta_{\rm op}$>0.1 for the compounds TA and TA+3H$^+$.

	Excited states	E/eV	$\lambda_{\rm op}$/nm	$\delta_{\rm op}$
TA	4	3.19	387.72	1.05
	5	3.19	387.70	1.04
	11	4.03	307.43	0.31
	12	4.03	307.42	0.31
			280*, 401*	
TA+3H$^+$	1	2.39	518.51	0.44
	2	2.39	518.15	0.44
	4	2.96	418.16	1.01
	5	2.96	418.06	1.01
	13	3.88	318.78	0.13
	14	3.88	318.75	0.13
			304*, 413*, 471*	

* The experimental results in Ref.[24].

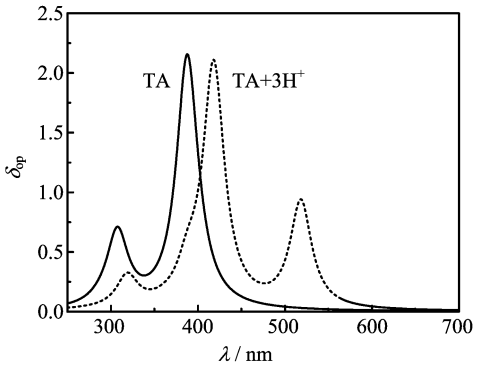

FIG. 2 The one-photon absorption spectra for the compounds TA and TA+3H$^+$.

absorbing wavelength in the interesting energy region attribute to the charge redistribution caused by the protonation as shown in Table II.

C. Two-photon absorption

The response theory on B3LYP level is applied to calculate TPA properties of the compounds. The calculated TPA cross sections of the ten lowest excited states are listed in Table IV. One can see that the maximal TPA cross sections for both the neutral TA and protonated TA+3H$^+$ appear at the sixth excited state, with 461.18 GM (GM=10^{-50} cm^{4}s/photon) at 705 nm and 669.49 GM at 815 nm, respectively. It is shown that the protonation enlarges the maximal TPA cross section of the molecule about 1.45 times. The TPA spectra of the TA and TA+3H$^+$ are shown in Fig.3. One can see that the TPA spectrum has an obvious red-shift after protonation. This feature demonstrates modulation of the protonation on the TPA property. For instance, when

DOI:10.1088/1674-0068/25/06/666-670

TABLE IV The TPA cross section σ_{tp}, the excitation energy E, and the corresponding two-photon wavelength λ_{tp} of the ten lowest excited states for the compounds TA and TA+3H$^+$.

TA			TA+3H$^+$		
E/eV	λ_{tp}/nm	σ_{tp}/GM	E/eV	λ_{tp}/nm	σ_{tp}/GM
2.97	832.30	5.54	2.39	1037.02	58.19
3.08	804.14	1.28	2.39	1036.30	58.67
3.08	803.96	1.33	2.72	909.38	0.10
3.19	775.44	86.09	2.96	836.32	58.24
3.19	775.40	86.09	2.96	836.12	58.05
3.51	705.10	461.18	3.03	815.76	669.49
		15.7 [24]			21.9 [24]
3.85	642.44	0.01	3.18	779.42	83.52
3.91	633.78	0.18	3.19	776.64	0.95
3.91	633.76	0.22	3.19	776.38	1.16
3.92	631.28	0.00	3.44	719.60	0.24

a laser with 700 nm is pumped on the molecules, there exists the maximal TPA cross section. If CF_3COOH solution is added into the molecular solution, resulting in protonation of the molecule, it is observed that the TPA cross section is very small. Therefore, the protonation and deprotonation operations result in switching of the two-photon absorption. Thus, a two-photon absorption switch with the compound TA based on the protonation effect may be realized.

According to the experimental measurement using a laser with wavelength of 800 nm, the TPA cross-sections of TA in neutral and acidic solution are 15.7 and 21.9 GM respectively, which approximately gives an increase of 1.39 times. It is observed that the theoretical calculations display qualitative agreement in the enhancement of the TPA cross-section with the experimental observations. However, the calculated values are quite larger than the experimental results. Except for the approximations of the theoretical methods, the discrepancy between theoretical and experimental results may be caused by the following points. The theoretical values are related to the two-photon resonant absorption and static condition. The experimental measurement may fail to tune the resonant condition. As one knows, the optical properties of the molecule are influenced by the interaction between light and molecules, namely, the measurement gives a dynamical value of the TPA cross-section. Furthermore, the long-range interaction in the solvent and the vibronic motions are not considered in the calculations.

D. Charge-transfer process

The charge in the molecule will be redistributed when the molecule is excited from the ground state to the CT state. For a better understanding of the charge transfer process, we visualize the charge density difference between the fourth CT and ground states before and after protonation using the Gaussview program as shown in Fig.4. When the compound TA is excited from the ground state to the fourth excited state, the main part of charge is accepted by the triazine core, and the two pyrrole groups donate the charge. When the compound TA is protonated, the charge transfer profile is modulated a lot. There exists charge transfer inside the triazine core.

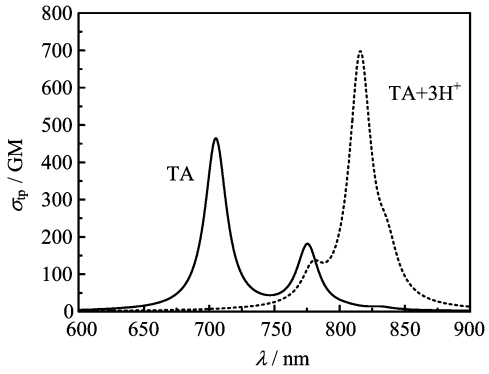

FIG. 3 The two-photon absorption spectra for the compounds TA and TA+3H$^+$.

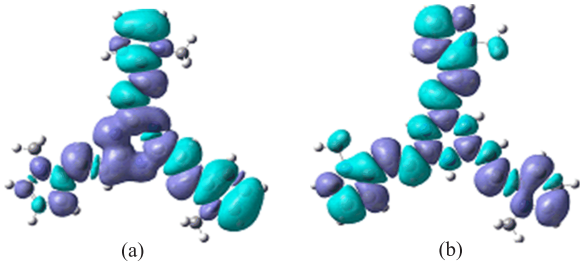

FIG. 4 The charge density difference between the forth excited state and the ground state of TA (a) and TA+3H$^+$ (b). The green and blue areas represent the electron loss and gain respectively. For interpretation of the color in this figure legend, the reader can refer to the web version of this article.

IV. CONCLUSION

When the tribranched chromophore TA with 1,3,5-triazine core and pyrrole electron-donating end-groups is in acid solution, the triazine N atoms will be protonated. The protonation effects on the optical properties of the chromophore have been investigated at DFT level. The response theory is used to calculate the two-photon absorption properties. The calculated results show that the protonation can enhance push-pull effect and induce more CT states in the interesting energy region, namely, more intramolecular charge transfer channels. The absorption band has a red-shift of wavelengths caused by the protonation. The large enhancement of the maximum two-photon absorption

DOI:10.1088/1674-0068/25/06/666-670

cross-section from 461.18 GM to 669.49 GM in the interesting energy region is observed after the protonation. The theoretical results are qualitatively consistent with the experimental measurement.

V. ACKNOWLEDGMENTS

This work was supported by the National Natural Science Foundation of China (No.10974121), the National Basic Research Program of China (No.2011CB808100), and the Natural Science Foundation of Shandong Province (No.ZR2010AZ002).

[1] M. Four, D. Riehl, O. Mongin, M. Blanchard-Desce, L. M. Lawson-Daku, J. Moreau, J. Chauvin, J. A. Delaire, and G. Lemercier, Phys. Chem. Chem. Phys. **13**, 17304 (2011).
[2] T. C. Lin, Y. J. Huang, Y. F. Chen, and C. L. Hu, Tetrahedron **66**, 1375 (2010).
[3] Q. Zheng, G. S. He, and P. N. Prasad, Chem. Phys. Lett. **475**, 250 (2009).
[4] X. Wang, J. Qiu, J. Song, J. Xu, Y. Liao, H. Sun, Y. Cheng, and Z. Xu, Opt. Commun. **280**, 197 (2007).
[5] G. Lemercier, J. C. Mulatier, C. Martineau, R. Anémian, C. Andraud, I. Wang, O. Stéphan, N. Amari, and P. Baldeck, C. R. Chim. **8**, 1308 (2005).
[6] M. Balaz, H. A. Collins, E. Dahlstedt, and H. L. Anderson, Org. Biomol. Chem. **7**, 874 (2009).
[7] S. C. Boca, M. Four, A. Bonne, B. v. d. Sanden, S. Astilean, P. L. Baldeck, and G. Lemercier, Chem. Commun. 4590 (2009).
[8] K. Ogawa and Y. Kobuke, Org. Biomol. Chem. **7**, 2241 (2009).
[9] T. Gallavardin, M. Maurin, S. Marotte, T. Simon, A. M. Gabudean, Y. Bretonnière, M. Lindgren, F. Lerouge, P. L. Baldeck, O. Stéphan, Y. Leverrier, J. Marvel, S. Parola, O. Maury, and C. Andraud, Photochem. Photobiol. Sci. **10**, 1216 (2011).
[10] X. Shen, L. Li, H. Wu, S. Q. Yao, and Q. H. Xu, Nanoscale **3**, 5140 (2011).
[11] Q. Zheng, G. S. He, T. C. Lin, and P. N. Prasad, J. Mater. Chem. **13**, 2499 (2003).
[12] J. D. Bhawalkar, G. S. He, C. K. Park, C. F. Zhao, G. Ruland, and P. N. Prasad, Opt. Commun. **124**, 33 (1996).
[13] C. C. Corredor, Z. L. Huang, K. D. Belfield, A. R. Morales, and M. V. Bondar, Chem. Mater. **19**, 5165 (2007).
[14] S. Engelhardt, Y. Hu, N. Seiler, D. Riester, W. Meyer, H. Krüger, M. Wehner, E. Bremus-Köbberling, and A. Gillner, J. Laser. Micro. Nanoeng. **6**, 54 (2011).
[15] K. S. Lee, R. H. Kim, D. Y. Yang, and S. H. Park, Prog. Polym. Sci. **33**, 631 (2008).
[16] W. Zhou, S. M. Kuebler, K. L. Braun, T. Yu, J. K. Cammack, C. K. Ober, J. W. Perry, and S. R. Marder, Science **296**, 1106 (2002).
[17] G. S. He, L. S. Tan, Q. Zheng, and P. N. Prasad, Chem. Rev. **108**, 1245 (2008).
[18] C. K. Wang, Z. Zhang, M. C. Ding, X. J. Li, Y. H. Sun, and K. Zhao, Chin. Phys. B **19**, 103304 (2010).
[19] Y. H. Sun, J. Li, K. Zhao, and C. K. Wang, Chin. Phys. B **19**, 044207 (2010).
[20] I. Asselberghs, K. Clays, A. Persoons, M. D. Ward, and J. McCleverty, J. Mater. Chem. **14**, 2831 (2004).
[21] M. H. V. Werts, S. Gmouh, O. Mongin, T. Pons, and M. Blanchard-Desce, J. Am. Chem. Soc. **126**, 16294 (2004).
[22] L. Antonov, K. Kamada, D. Nedeltcheva, K. Ohta, and F. S. Kamounah, J. Photochem. Photobiol. A **181**, 274 (2006).
[23] I. Asselberghs, G. Hennrich, and K. Clays, J. Phys. Chem. A **110**, 6271 (2006).
[24] L. Liu, Z. Zhou, J. Shi, Z. Liu, C. Lu, W. He, J. Ma, Y. Cui, and G. Y. Lu, Synth. Met. **161**, 783 (2011).
[25] M. M. Oliva, J. Casado, J. T. L. Navarrete, G. Hennrich, M. C. R. Delgado, and J. Orduna, J. Phys. Chem. C **111**, 18778 (2007).
[26] C. Cardoso, P. E. Abreu, and F. Nogueira, J. Chem. Theory Comput. **5**, 850 (2009).
[27] M. C. Ding, Z. Zhang, Y. Song, and C. K. Wang, Chin. J. Chem. Phys. **23**, 664 (2010).
[28] M. J. Frisch, G. W. Trucks, H. B. Schlegel, G. E. Scuseria, M. A. Robb, J. R. Cheeseman, J. A. Jr. Montgomery, T. Vreven, K. N. Kudin, J. C. Burant, J. M. Millam, S. S. Iyengar, J. Tomasi, V. Barone, B. Mennucci, M. Cossi, G. Scalmani, N. Rega, G. A. Petersson, H. Nakatsuji, M. Hada, M. Ehara, K. Toyota, R. Fukuda, J. Hasegawa, M. Ishida, T. Nakajima, Y. Honda, O. Kitao, H. Nakai, M. Klene, X. Li, J. E. Knox, H. P. Hratchian, J. B. Cross, C. Adamo, J. Jaramillo, R. Gomperts, R. E. Stratmann, O. Yazyev, A. J. Austin, R. Cammi, C. Pomelli, J. W. Ochterski, P. Y. Ayala, K. Morokuma, G. A. Voth, P. Salvador, J. J. Dannenberg, V. G. Zakrzewski, S. Dapprich, A. D. Daniels, M. C. Strain, Ö. Farkas, D. K. Malick, A. D. Rabuck, K. Raghavachari, J. B. Foresman, J. V. Ortiz, Q. Cui, A. G. Baboul, S. Clifford, J. Cioslowski, B. B. Stefanov, G. Liu, A. Liashenko, P. Piskorz, I. Komaromi, R. L. Martin, D. J. Fox, T. Keith, M. A. Al-Laham, C. Y. Peng, A. Nanayakkara, M. Challacombe, P. M. W. Gill, B. Johnson, W. Chen, M. W. Wong, C. Gonzalez, and J. A. Pople, *Gaussian* 03, *Revision B*.01, Pittsburgh, PA: Gaussian Inc., (2003).
[29] DALTON, A Molecular Electronic Structure Program, Release Dalton2011 (2011), http://daltonprogram.org/.
[30] G. P. Zhang, G. C. Hu, Z. L. Li, and C. K. Wang, J. Phys. Chem. C **116**, 3773 (2012).

DOI:10.1088/1674-0068/25/06/666-670